

**UNIVERSITY OF SZEGED**  
FACULTY OF SCIENCE AND INFORMATICS  
**DOCTORAL SCHOOL OF GEOSCIENCES**  
DEPARTMENT OF GEOINFORMATICS, PHYSICAL AND  
ENVIRONMENTAL GEOGRAPHY

**A MULTI-SCALE INVESTIGATION OF  
SEDIMENT AND PLASTIC POLLUTION  
TRANSPORT IN THE TISZA RIVER  
APPLYING REMOTE SENSING AND MACHINE  
LEARNING: A HYDROLOGICAL PERSPECTIVE**

Ph.D. Dissertation

**Ahmed Mohsen Abdelsadek Metwaly**

SUPERVISORS:

DR. TÍMEA KISS (DSc), Associate Professor

DR. FERENC KOVÁCS, Associate Professor

**SZEGED**  
**2024**

## 1. INTRODUCTION

Rivers are the main conveyors of terrestrial plastic pollution, including macroplastics (MaP) and microplastics (MP) to marine environments. However, they also act as reservoirs, influenced by intricate hydrological, meteorological, and morphological factors. The actual role of rivers in riverine plastic pollution, the spatiotemporal dynamics of the contamination, its influencing factors, and transport mechanisms are still understudied and have many contradictory results. In this respect, extensively studied sediment transport can provide valuable concepts and theories for a better understanding of riverine plastic pollution transport, particularly by analyzing the connection between suspended sediment (SS) and MP transport. However, existing studies often examine them individually or assess their correlations based on limited spatiotemporal measurements, leading to unreliable and conflicting findings.

The SS and MP particles share similar physical characteristics and are transported from the catchment to the river channel through the same mechanism. However, the disparity of their sources and the various densities of plastics may lead to dissimilar behavior in their responses to various temporal and longitudinal variables and consequently disparate spatiotemporal distributions. For instance, the response of MP and SS transport to changes in hydrological condition (e.g., low stages, rising, peak, and falling phase of floods), as well as to longitudinal variables e.g., dams and tributaries may differ. However, these aspects have not been examined so far. Furthermore, no study has investigated the influence of hydrological parameters of a tributary and mainstream on the water mixing process in a confluence area, a critical factor influencing downstream transport of SS and MP.

The study of SS, MaP, and MP transport in rivers relies on intensive spatiotemporal in-situ measurements, which are costly, time-consuming, and labor-intensive. Besides, they face a global decline in funding for monitoring programs. These could be partially solved by remote sensing techniques using satellite sensors, owing to their large-scale coverage and frequent monitoring, even for remote or inaccessible river sections. However, this scientific field is still in its early stages, with many conflicting results, especially in the context of MaP and MP transport.

Most previous studies developed remote sensing-based MaP, SS, and MP concentration models and relied on measured water discharge ( $Q$ ) to determine their transport rates. However, the monitoring of  $Q$  in

many rivers and river sections is often limited or missing. Some studies have attempted to integrate remote sensing data with existing hydraulic or hydrological models for  $Q$  estimation; however, this approach demands extensive hydrological, hydraulic, meteorological, and morphological data, which may not always be available. Integrating hydraulic geometry theory with remote sensing data may provide an efficient and cost-effective alternative for  $Q$  estimation, yet this approach has achieved only moderate to low estimation accuracy; thus, it requires further refinement.

Remote sensing of MP concentration in aquatic environments is still questionable owing to its subtle contribution to sensor signals. Yet, MaP particles are detectable, though the technical characteristics of the employed satellite sensor and the sub-pixel detection are still inadequately studied. Notably, most of the previous studies focused on oceans to develop satellite-based MaP and MP models, while very few were elaborated on rivers and for MaPs only. Besides, no study has explored the potential use of active water constituents, mainly SSC, as a potential proxy for MP concentration; though, this approach could address challenges associated with the direct detection of MP concentration by satellite sensors.

Several studies employed different approaches for MaP detection, including bio-optical modelling, indices, and deep learning. However, these approaches require abundant auxiliary data and a large MaP dataset, which is often unavailable. Therefore, there is a necessity for developing MaP models based on traditional machine learning algorithms [e.g., support vector machine (SVM) and random forest (RF)], as these algorithms require less extensive data.

## 2. OBJECTIVES AND GOALS

The main objective of this study is to evaluate the transport dynamics of SS and plastic pollution (MP and MaP) in rivers across multiple spatiotemporal scales. The study involves a comparative analysis of their influencing factors and the development of satellite-based models to support future monitoring programs.

The goals of the study are:

- To investigate the spatiotemporal distribution of MaP in the Tisza River based on in-situ observations and satellite images.
- To develop Sentinel-2-based MaP models utilizing VHR images from Google Earth Satellites and machine learning algorithms.
- To develop Sentinel-2-based  $Q$  models by integrating hydraulic

geometry theory with machine learning algorithms.

- To develop Sentinel-2-based SSC models utilizing long time series of SSC measurements and machine learning algorithms to estimate sediment discharge ( $Q_s$ ) in rivers.
- To investigate the influence of hydrological parameters of joining rivers on the water mixing process in the Tisza–Maros confluence area.
- To reveal the spatiotemporal distribution and correlation of surficial SS and MP concentrations in the Tisza River based on intensive in-situ measurements and satellite images.
- To compare the influence of dams and tributaries in the transport of surficial SS and MP in the Tisza River.
- To evaluate the potential of various satellite sensors (Sentinel-2, PlanetScope, and Sentinel-1) to estimate MP concentration directly and indirectly through surficial SSC as a proxy.

### **3. DATA COLLECTION AND METHODS**

#### ***3.1 Derivation of remote sensing-based riverine litter and MaP models and revealing its spatiotemporal distribution in the Tisza River***

Riverine litter spots, including MaPs, were investigated in the Tisza River by in-situ observations in Szeged (February 18<sup>th</sup> and 23<sup>rd</sup>; and March 5<sup>th</sup> and 10<sup>th</sup>, 2021) and by analyzing 13 VHR images from Google Earth Satellites. Concurrent 16 Sentinel-2 images for the identified spots were employed to train and validate five machine learning algorithms [i.e., decision tree (DT), naïve bayes (NB), artificial neural network (ANN), RF, and SVC] to derive riverine litter models. The generalization capability of the developed models was tested on litter spots with varying sizes ( $\leq 1$  pixel to  $\geq 4$  pixels). The best-derived model was utilized to investigate the spatiotemporal dynamics of riverine litter in the Middle Tisza (276–451 river km) and assess its temporal trend over a seven-year study period (2015–2021), applying the seasonal Mann-Kendall trend analysis test.

#### ***3.2 Derivation of remote sensing-based suspended sediment discharge models and revealing its spatiotemporal distribution in the Tisza and Maros Rivers***

Remote sensing-based models were developed for both components of  $Q_s$ , including  $Q$  and SSC. The models were based on monthly  $Q$  and SSC in-situ measurements in the Lower Tisza (at Algyó and Szeged) and Maros Rivers (at Makó) (Figure 1B) and concurrent Sentinel-2 images (Tisza: 29 images; Maros: 27 images; 2015–2020).

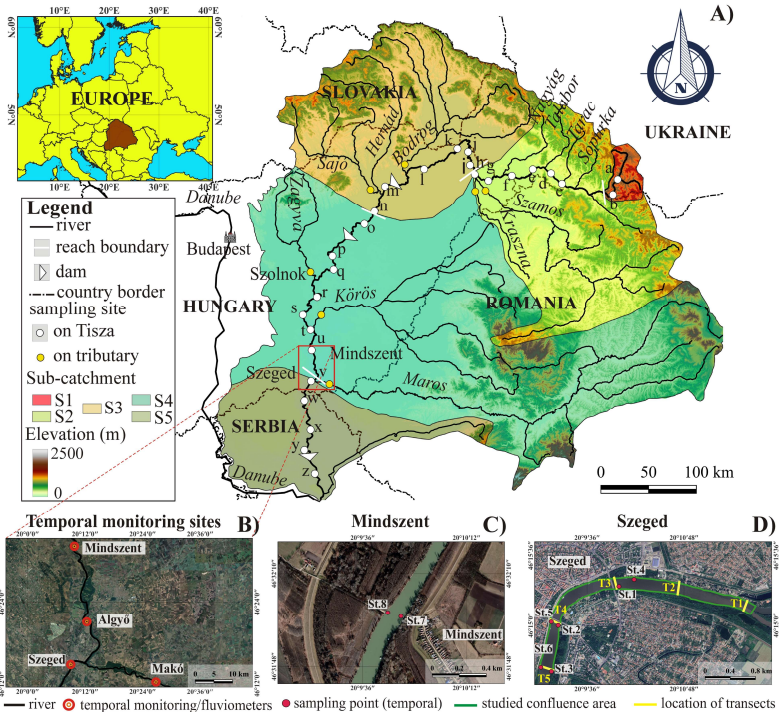


Figure 1. The catchment of the Tisza River and locations of the measuring sites during spatiotemporal measurements.

For  $Q$  modelling, the at-a-station hydraulic geometry (AHG) power law and at-many-station hydraulic geometry (AMHG) methods were applied based on river width data (at the three gauging sites) obtained from Sentinel-2 images and concurrent in-situ  $Q$  measurements. Furthermore, a novel AHG machine learning method was developed, combining hydraulic geometry theory with machine learning algorithms (ANN, SVM, RF, and their combination). Similarly, SSC models were developed by conducting a regression between the reflectance of Sentinel-2 bands (B2–B8a) and measured SSCs along the cross sections in Szeged (Tisza) and Makó (Maros) employing the same algorithms. The best-derived  $Q$  and SSC models were integrated to investigate  $Q_s$  dynamics in the Lower Tisza and Maros Rivers over an extended period (July 2015–May 2021) using 93 Sentinel-2 images.

### ***3.3. Investigation on the influence of hydrology on the water mixing process in the Tisza–Maros confluence area***

The mixing process of the water of the Tisza and Maros and its relationship to the hydrology of the joining rivers were investigated in detail by 143 Sentinel-2 images, daily measurements of water stage ( $H$ ) and  $Q$  at the three gauging sites (i.e., Algyó, Szeged and Makó; Figure 1B) from July 2015 to May 2021. The K-means classification technique was applied to classify water pixels in the confluence area into Tisza water (TW), Maros water (MW), and their mixture (MIX). Additional hydrological parameters were calculated (e.g.,  $Q$  and slope difference between the joining rivers, as well as their ratio). The strength of the correlation between measured and calculated hydrological parameters and the areal coverage (%) of TW, MW, and MIX along with the longitudinal extent of the MW into the Tisza ( $L$ ) was tested by the Pearson correlation test. The lateral mixing was examined by estimating the percentage of TW, MW, and MIX coverage at five transects (Figure 1D) relative to the corresponding river width. To support future sampling campaigns in the confluence area, predictive equations for TW, MW, MIX, and  $L$  were developed based on hydrological parameters at the gauging sites.

### ***3.4. Investigating the spatiotemporal distribution and correlation of surficial suspend sediment and microplastic concentrations in the Tisza***

The spatiotemporal distribution and correlation of surficial SS and MP concentrations in the Tisza River were evaluated based on intensive spatial (26 sites in August 2021, and 21 sites in July 2022; Figure 1A) and temporal (140 samples in Mindszent from May 2021 to May 2023; Figure 1C) measurements. Remarkably, such intensive measurements were applied for the first time in rivers globally, enhancing the reliability of the results and their contribution to the existing scientific knowledge. The SSC was measured by the evaporation method; while the MP concentration by density separation, digestion, ATR-FTIR, and visual identification. The temporal dynamics and correlation of surficial SS and MP concentrations were analyzed collectively considering all hydrological conditions, and individually for low stages, flood waves (minor and medium floods), and flood phases (i.e., rising, peak, and falling phases). The study also assessed their dynamics and correlation along the river sections (S1–S5) and in response to longitudinal factors, such as dams and tributaries. Parametric and non-parametric tests were applied to evaluate potential statistical differences in their distribution in space and time.

### ***3.5. Derivation of remote sensing-based surficial suspended sediment and microplastic concentration models***

The previously introduced intensive in-situ surficial SS and MP concentration measurements were complemented with additional SSC measurements in Szeged (St.1–6; Figure 1D), and concurrent Sentinel-2 (137 images), PlanetScope (177 images) and Sentinel-1 (239 images) images to derive surficial SS and MP concentration models. The correlation between surficial SS and MP concentrations, as well as the reflectance and backscattering of the images, was tested, and then the MLP neural network was used to establish their direct models. Furthermore, proxy models for MP concentration were developed based on SSC, considering all hydrological conditions and individually (i.e., low stages, rising, peak, and falling phases of floods). The generalization capability of the derived models was tested across various hydrological scenarios and along the Tisza, between Aranyosapáti (site “i”) and Tiszaroff (site “p”) (Figure 1A).

## **4. RESULTS**

### ***4.1 Spatiotemporal distribution of riverine litter and macroplastics in the Tisza River***

*Macroplastics constitute a low proportion of the riverine litter in the Tisza River and exhibit slightly different transport rates; however, both are highly influenced by hydrology.*

Most of the riverine litter had an organic origin owing to the continuous input of organic debris, especially at meandering sections with high bank erosion. Meanwhile, the litter contains only 5–20% MaPs, consistent with existing literature. The Tisza showed a comparable riverine litter transport rate (mean: 156 spot/h) to rivers globally, as well as a positive correlation with  $H$  and  $Q$  changes. This pattern was characteristic to MaP transport too (123 item/h), though it showed a weaker association with  $H$  and  $Q$ . This suggests potential differences in their sources, influencing factors, and transport mechanisms.

*The longitudinal distribution of riverine litter is closely related to waste management practices in sub-catchments, although it may be influenced by local sources and/or the trapping effect of hydraulic structures.*

Elevated riverine litter transport was observed in the Upper Tisza owing to high communal waste production and low recycling ratio in these regions, with a subsequent decline downstream. However, this spatial pattern is highly influenced by the trapping effect of hydraulic

structures and local anthropogenic activities/sources (illegal waste disposals, fishing, and tourist activities). For instance, a significant proportion of riverine litter was observed upstream of dams, bridges, and around docks, regardless of applied waste management practices in sub-catchments. Furthermore, the density of riverine litter (1.2–1.6 spot/km) downstream of the Kisköre Dam was higher than upstream of the dam (0.85–1 spot/km), indicating the influence of potential local riverine litter sources downstream.

*Although the highest riverine litter transport rate usually occurs during flood waves, it is recommended to conduct the purification campaigns at the end of the flood period, when litter accumulates with the largest area at hot spots under the influence of gradual flux.*

The largest riverine litter spot developed upstream of the Kisköre Dam, and it occurred at the end of the summer flood. Thus, it was probably formed as a result of gradual accumulation over successive flood waves. The statistical analysis revealed a rising trend in the area of this litter spot over the seven-year study period. It is probably attributed to the absence of significant, overbankfull floods during this timeframe, and the increasing waste input into the river.

#### ***4.2 Remote sensing-based riverine litter and macroplastic modelling: opportunities and limitations***

*The NIR and SWIR spectral bands are the most suitable for detecting riverine litter. Besides, the integration of spectral indices into the development of riverine litter models may enhance their performance.*

Based on spectral and SHAP analysis, the NIR and SWIR bands, especially B8, B11, and B12 in the Sentinel-2 sensor, are the most suitable to develop remote sensing-based riverine litter models, as riverine litter had a distinct spectral signature within this range compared to river water and obstructions. The integration of spectral indices, especially the plastic index (PI), normalized difference water index (NDWI), and normalized difference vegetation index (NDVI), enhances the estimation accuracy of the models, though the floating debris index (FDI) showed a slight influence.

*The derived riverine litter models showed good and comparable evaluation metrics, with superior performance achieved by SVC, ANN, and RF, while DT and NB demonstrated comparatively lower accuracy.*

The potential of traditional machine learning algorithms in dealing

with intricate, non-linear problems with limited datasets, resulted in accurate riverine litter models with comparable evaluation metrics, as the F1-score ranged between 0.83 (NB) and 0.94 (SVC). However, it must be noted that additional data are still required to enhance the robustness and reliability of the models, as during the testing phase on a larger dataset, the F1-score declined to 0.45 (DT)–0.69 (RF). Based on the validation and testing of the five algorithms, the SVC, ANN, and RF are the most recommended for future riverine litter modelling, as they achieved the highest metrics and the best performance on several spot sizes. Meanwhile, the DT and NB are less recommended, as the DT occasionally misclassifies river water as litter, and NB struggles to distinguish between litter and obstructions.

*The models achieved high performance with large and medium spots, while the detection of small spots (sub-pixel) is still questionable.*

The strong reflectance associated with large and medium litter spots enabled the models to detect them effectively, though they slightly over (large spot) or underestimated (medium spot with SVC) their area. On the other hand, the low reflectance of small spots hindered sub-pixel detection for all models except for NB. However, NB's detection is uncertain owing to its relatively lower estimation accuracy and challenges in discriminating riverine litter from obstructions. Therefore, further studies in sub-pixel detection are warranted, incorporating larger small litter spots, as they formed only 1% of the employed dataset in this study.

#### ***4.3 Remote sensing-based suspended sediment discharge modelling: opportunities and limitations***

*The highest  $Q_s$  usually occur during flood waves and the lowest during low stages in both the Tisza and Maros Rivers. Moreover, clockwise hysteresis in the SSC– $Q$  relationship is more likely to occur in the Tisza than in the Maros.*

The Maros River showed a two-fold higher mean SSC ( $129 \text{ g/m}^3$ ) than the Tisza ( $58 \text{ g/m}^3$ ); however, it transported 2–3.5 lower  $Q_s$  (Maros:  $1264 \text{ t/day}$ ; Tisza:  $2584 \text{ t/day}$ ) due to its lower discharge ( $157 \text{ m}^3/\text{s}$ ) than the Tisza ( $702 \text{ m}^3/\text{s}$ ). The peaks and slumps of  $Q_s$  of the rivers do not necessarily coincide. For instance, during the largest flood wave in 2016 (study period: 2015–2020), the  $Q_s$  peak occurred in the Tisza during the early spring flood in March, while the Maros experienced its peak during the early summer flood in June. Typically, the Tisza exhibits a clockwise hysteresis in the SSC– $Q$  relationship due

to the availability and proximity of sediment sources at the onset of flood waves. However, this phenomenon was less likely to occur in the Maros, as indicated also by the higher Pearson correlation coefficient ( $r$ ) between SSC and  $Q$  in the Maros (0.88) compared to the Tisza (0.72).

*The lateral distribution of SSC at river-cross sections is influenced by the distribution of lateral flow velocity and by the presence and location of an upstream tributary.*

The lateral distribution of SSC in the monitoring cross-section (used by the ATIVIZIG) of the Tisza at Szeged showed greater variability than its counterpart in the Maros at Makó. This variability was more pronounced during floods than during low stages in both cross sections. Typically, the highest SSC in the Makó cross-section aligns with the thalweg (highest flow velocity). Meanwhile, in Szeged, the highest SSC is typical in the low-velocity field on the left bank, as the monitoring location is just 4.2 km downstream of the Tisza–Maros’s confluence, where the rivers' waters are still mixing.

*The integration of hydraulic geometry theory, particularly the water width– $Q$  relationship, with remote sensing data and machine learning algorithms could offer a cost-effective, reliable, and recurring monitoring method for  $Q$  in rivers.*

The AMHG  $Q$  models exhibited higher estimation accuracy (mean:  $R^2=0.62$ ;  $RMSE=172 \text{ m}^3/\text{s}$ ) than the AHG power law models (mean:  $R^2=0.57$ ;  $RMSE=645 \text{ m}^3/\text{s}$ ). However, the developed AHG machine learning models surpassed both methods (mean:  $R^2=0.7$ ;  $RMSE=140 \text{ m}^3/\text{s}$ ). Remarkably, the models generally provide accurate estimates below the bankfull level but could overestimate (e.g., AHG power law) or underestimate (e.g., AMHG) real  $Q$  values above the bankfull level, due to losing hydraulic geometry characteristics. However, the AHG machine learning method partially addressed this issue. It is noteworthy that the estimation accuracy of the models is significantly influenced by the river’s cross-section shape and size. Certain shapes (e.g., V-shape) have better hydraulic geometry than others (e.g., trapezoidal shape), and width estimates in wide cross sections have higher accuracy than narrow ones. Therefore, the wide, V-shaped cross-sections in Szeged and Algyő exhibited higher accuracy in  $Q$  estimates than the narrow, trapezoidal cross-section in Makó.

*Integrating Sentinel-2 images with in-situ measurements of SSC through machine learning algorithms yielded accurate SSC models; however, it is important to consider their limitations.*

The derived Sentinel-2-based SSC models in the Tisza and Maros Rivers showed high and comparable accuracy, with slightly better performance in the Maros ( $R^2=0.85$ ) than the Tisza ( $R^2=0.8$ ). Remarkably, the spectral analysis highlighted the suitability of the 560 nm wavelength (B3 in Sentinel-2) for estimating low SSC and 704 nm (B5) for high SSCs. Among the three tested algorithms (RF, ANN, and SVC), RF exhibited the best performance, making it highly recommended for future studies. The best-performed SSC and  $Q$  models effectively depicted the  $Q_s$  transport in the Lower Tisza and Maros Rivers, not only longitudinally, but also laterally and during various hydrological conditions. However, the  $Q_s$  estimates near the riverbanks should be interpreted with caution, as the reflectance of these mixed pixels is influenced by both water and land.

#### ***4.4 Spatiotemporal dynamics of water mixing in the Tisza–Maros confluence in response to hydrology: support for future measurements***

*The Maros River showed greater variations in water stage and slope conditions than the Tisza and its hydrological condition is highly influenced by the impoundment impact, especially during floods.*

Based on calculated hydrological parameters in the Tisza and Maros Rivers, the Maros exhibited faster rising (145 cm/day) and falling (–151 cm/day) rates, and a wider slope range (2.7–19.6 cm/km) throughout the study period. This indicates the flashy regime of the Maros compared to the Tisza. Notably, the greatest  $Q$  contribution of the Maros to the Tisza (37–57%) typically occurs during low stages, when its elevated slope enables it to overcome the impoundment effect of the Tisza. Meanwhile, this contribution declines significantly during floods (6–10%) due to the elevated stream power of the Tisza and the impoundment effect.

*Hydrological parameters considerably influence the dynamism of water mixing in the confluence area, especially the discharge ratio between the joining rivers is important. The water types (i.e., TW, MW, and MLX) predominated under distinct hydrological conditions and in specific periods.*

Based on the Pearson correlation analysis, the most influential hydrological parameters in the water mixing process include the discharge ratio ( $Q_{\text{Makó}}/Q_{\text{Szeged}}$ ), slope (S), and slope difference ( $S_{\text{Tisza}} - S_{\text{Maros}}$ ). In contrast, the least influential parameters are daily water stage

difference ( $\Delta H$ ) and its variance between the joining rivers ( $\Delta H_{\text{Algyő}} - \Delta H_{\text{Makó}}$ ). While the  $S$  and  $S_{\text{Tisza-SMaros}}$  showed better correlations under separating flood waves from low stages, the  $Q_{\text{Makó}}/Q_{\text{Szeged}}$  showed the highest correlations regardless of the hydrological condition. Based on the analyzed 143 Sentinel-2 images, the full coverage of TW usually occurs during floods when the Tisza impounds the Maros. In exceptional cases, MW may govern the confluence area during simultaneous floods in both rivers, associated with elevated stream power of the Maros to overcome the impoundment effect of the Tisza. The MIX water generally prevails during low stages in summer and has almost no coverage during floods.

*The water mixing process in the confluence area was categorized into 11 mixing patterns, and predictive equations for mixing water variables (i.e., TW, MW, MIX, and L) were developed based on rivers' hydrology.*

Eleven mixing patterns were identified in the confluence area based on the dominance of each water type (TW, MW, and MIX) and their likelihood of downstream upwelling due to density differences. Besides, the characteristic period and probability of occurrence of each pattern were unveiled. In support of future SS or MP monitoring measurements in the confluence area, predictive equations for mixing water variables (TW, MW, MIX, and L) were developed based on measured and calculated hydrological parameters in three gauging sites (Szeged, Algyő, and Makó) with a moderate to strong accuracy ( $R^2=0.4-0.82$ ). Unfortunately, the complexity of the mixing process in the confluence area impedes better accuracy to be achieved.

#### ***4.5 Spatiotemporal distribution and correlation of surficial suspended sediment and microplastic concentrations in the Tisza River in response to the river's hydrology and longitudinal variables***

*Hydrology considerably influences the temporal dynamics of surficial SS and MP transport, with a stronger influence on SS than MPs. Sources and factors for MP differ from SS in low stages but converge during floods, as evidenced by correlation analysis.*

The lowest concentrations of surficial SS and MP were recorded during low stages ( $SS_{\text{low}}: 34 \pm 14 \text{ g/m}^3$ ;  $MP_{\text{low}}: 21 \pm 16 \text{ item/m}^3$ ) and the highest concentrations during flood waves ( $SS_{\text{medium}}: 97 \pm 75 \text{ g/m}^3$ ;  $MP_{\text{medium}}: 47 \pm 27 \text{ item/m}^3$ ). However, correlation analysis revealed a stronger correlation between surficial SSC and water stage ( $H$ ) ( $\rho_{SS-H}=0.7$ ) compared to MP ( $\rho_{MP-H}=0.5$ ). This discrepancy suggests a higher

complexity of MP transport than of SS, and the involvement of additional factors influencing MP transport. Remarkably, a strong positive correlation ( $\rho_{SS-MP}=0.6$ ) was found between surficial SS and MP concentrations considering all hydrological conditions. Meanwhile, the separation of the individual conditions revealed a robust correlation during flood waves and negligible correlation during low stages. This finding may suggest that the sources of SS and MPs during low stages are dissimilar, while during flood waves new sources common for both variables (e.g., runoff and mobilization of deposited SS and MP from the channel) appear in the system. The analysis also highlighted the importance of event sequence in SS and MP transport, as the rising phase and first flood waves typically transport higher loads than the falling phase and subsequent waves.

*The longitudinal distribution of surficial SSC varied from MP's along the river sections, with no discernible evidence of a downstream trend.*

The surficial SS and MP concentrations exhibited similar distribution patterns along the river sections (S1–5; Figure 1A) in both measuring years, with higher magnitudes observed in 2022. However, they differed from each other, with no clear downstream trend. The most polluted sections with MP were in the Upper (S1) and Lower (S5) Tisza, while the Middle Tisza (S3–S4) was the least polluted. Conversely, the highest SSCs were recorded in the Middle Tisza (S3–S4) and the lowest in the Lower Tisza (S5). Accordingly, a moderate negative correlation was identified between both variables (i.e., surficial SS and MP concentrations) in both years (2021:  $\rho_{SS-MP}$ :  $-0.35$ ; 2022:  $\rho_{SS-MP}$ :  $-0.41$ ). This longitudinal distribution and correlation suggest that both variables may have dissimilar sources and/or influencing factors during low stages. However, further sampling during floods is warranted to gain deeper insights and draw a comprehensive picture of their transport process.

*Tributaries and dams exert a profound influence on surficial SS and MP transport in the Tisza. However, they revealed a more consistent influence on SS transport than MP's.*

Tributaries exhibited three-fold higher surficial SS and 1.2-fold higher MP concentrations than the Tisza; however, their influence on the Tisza was closely related to the  $Q$  of the tributary. Notably, they showed dissimilar influences on SS and MP concentrations downstream of their confluences. The Kraszna (concentrating) and the Zagyva (diluting) were the only tributaries that influenced the surficial SS and

MP concentrations equally in both years; meanwhile, the rest of the tributaries revealed temporally different influences. Dams, on the other hand, tended to stimulate SS deposition upstream in their reservoirs and induce clear water erosion downstream. Meanwhile, ambiguous patterns were noticed in the MP concentrations not only along the three reservoirs of the Tisza but also temporally.

#### ***4.6 Remote sensing-based surficial suspended sediment and microplastic concentration modelling: opportunities and limitations***

*Surficial SSC exhibited stronger correlations with the optical sensors than MP concentration, while both variables showed negligible correlations with the active sensor's channels.*

Correlation and spectral analysis revealed that the reflectance of optical sensors is less influenced by MP concentration than surficial SSC; however, backscattering of active sensors is influenced by neither variable. Among the optical sensors, surficial SSC showed the highest correlation with the Sentinel-2 bands, while MP concentration was with the PlanetScope bands. Remarkably, bands B4 and B5 in Sentinel-2 and their counterparts B6 and B7 in PlanetScope were the most correlated bands with surficial SS and MP concentrations. However, these correlations exhibited a non-linear relationship, emphasizing the necessity of utilizing regression techniques capable of dealing with non-linearly correlated datasets for developing their models.

*Direct estimation of surficial SSC by optical sensors is achievable with high accuracy, meanwhile, it remains questionable for MP concentration. Yet, proxy models based on active water constituents (e.g., SSC) may serve as an adequate alternative for MP concentration estimation.*

The direct Sentinel-2-based surficial SSC model exhibited higher accuracy ( $R^2=0.7$ ) than the PlanetScope-based model ( $R^2=0.6$ ). Meanwhile, both sensors revealed low accuracy for MP concentration estimation (Sentinel-2:  $R^2=0.0$ ; PlanetScope:  $R^2=0.2$ ). This is likely attributed to the low concentration levels of MPs in rivers, their transport just below the water surface, and the limited spatial and spectral characteristics of the tested sensors. On the other hand, the proxy MP concentration models based on SSC revealed promising results, especially during floods ( $R^2=0.8$ ). However, it is important to consider their limitations, as these models may offer less accurate estimates during low stages, and the established relationship should be recurrently calibrated.

## PUBLICATIONS RELATED TO THE DISSERTATION

- Mohsen, A., Kovács, F., Mezősi, G., Kiss, T., 2021.** Sediment Transport Dynamism in the Confluence Area of Two Rivers Transporting Mainly Suspended Sediment Based on Sentinel-2 Satellite Images. *Water*, 13(21): 3132. DOI: <https://doi.org/10.3390/w13213132> (Impact factor: 3.103)
- Mohsen, A., Kovács, F., Kiss, T., 2022.** Remote Sensing of Sediment Discharge in Rivers using Sentinel-2 Images and Machine-learning Algorithms. *Hydrology*, 9(5): 88. DOI: <https://doi.org/10.3390/hydrology9050088> (Impact factor: 3.2)
- Balla, A., Mohsen, A., Gönczy, S., Kiss, T., 2022.** Spatial Variations in Microfiber Transport in a Transnational River Basin. *Applied Sciences*, 12(21): 10852. DOI: <https://doi.org/10.3390/app122110852> (Impact factor: 2.7)
- Mohsen, A., Kiss, T., Kovács, F., 2023.** Machine learning-based Detection and Mapping of Riverine Litter Utilizing Sentinel-2 Imagery. *Environmental Science and Pollution Research*, 30(25): 67742-67757. DOI: <https://doi.org/10.1007/s11356-023-27068-0> (Impact factor: 5.7)
- Mohsen, A., Balla, A., Kiss, T., 2023.** High Spatiotemporal Resolution Analysis on Suspended Sediment and Microplastic Transport of a Lowland River. *Science of The Total Environment*, 902: 166188. DOI: <https://doi.org/10.1016/j.scitotenv.2023.166188> (Impact factor: 9.8)
- Mohsen, A., Kovács, F., Kiss, T., 2023.** Riverine Microplastic Quantification: A Novel Approach Integrating Satellite Images, Neural Network, and Suspended Sediment Data as a Proxy. *Sensors*, 23(23): 9505. DOI: <https://doi.org/10.3390/s23239505> (Impact factor: 3.84)

## Co-author's declaration

As a co-author of the following publications, I formally declare that the jointly published findings in both the thesis and the publications are greatly contributed by the candidate and were not or will not be used in the past or the future, respectively, for the purpose of acquiring an academic degree or title.

- Sediment Transport Dynamism in the Confluence Area of Two Rivers Transporting Mainly Suspended Sediment Based on Sentinel-2 Satellite Images. DOI: <https://doi.org/10.3390/w13213132>
- Remote Sensing of Sediment Discharge in Rivers using Sentinel-2 Images and Machine-learning Algorithms. DOI: <https://doi.org/10.3390/hydrology9050088>
- Spatial Variations in Microfiber Transport in a Transnational River Basin. DOI: <https://doi.org/10.3390/app122110852>
- Machine learning-based Detection and Mapping of Riverine Litter Utilizing Sentinel-2 Imagery. DOI: <https://doi.org/10.1007/s11356-023-27068-0>
- High Spatiotemporal Resolution Analysis on Suspended Sediment and Microplastic Transport of a Lowland River. DOI: <https://doi.org/10.1016/j.scitotenv.2023.166188>
- Riverine Microplastic Quantification: A Novel Approach Integrating Satellite Images, Neural Network, and Suspended Sediment Data as a Proxy. DOI: <https://doi.org/10.3390/s23239505>

Szeged

January 3<sup>rd</sup>, 2024.

Dr. TÍMEA KISS



.....

## Co-author's declaration

As a co-author of the following publications, I formally declare that the jointly published findings in both the thesis and the publications are greatly contributed by the candidate and were not or will not be used in the past or the future, respectively, for the purpose of acquiring an academic degree or title.

- Sediment Transport Dynamism in the Confluence Area of Two Rivers Transporting Mainly Suspended Sediment Based on Sentinel-2 Satellite Images. DOI: <https://doi.org/10.3390/w13213132>
- Remote Sensing of Sediment Discharge in Rivers using Sentinel-2 Images and Machine-learning Algorithms. DOI: <https://doi.org/10.3390/hydrology9050088>
- Machine learning-based Detection and Mapping of Riverine Litter Utilizing Sentinel-2 Imagery. DOI: <https://doi.org/10.1007/s11356-023-27068-0>
- Riverine Microplastic Quantification: A Novel Approach Integrating Satellite Images, Neural Network, and Suspended Sediment Data as a Proxy. DOI: <https://doi.org/10.3390/s23239505>

Szeged

January 5<sup>th</sup>, 2024.

DR. FERENC KOVÁCS



## Co-author`s declaration

As a co-author of the following publication, I formally declare that the jointly published findings in both the thesis and the publication are greatly contributed by the candidate and were not or will not be used in the past or the future, respectively, for the purpose of acquiring an academic degree or title.

- Sediment Transport Dynamism in the Confluence Area of Two Rivers Transporting Mainly Suspended Sediment Based on Sentinel-2 Satellite Images. DOI: <https://doi.org/10.3390/w13213132>

Szeged

January 3<sup>rd</sup>, 2024.

Prof. Dr. GÁBOR MEZŐSI



## Co-author`s declaration

As a co-author of the following publication, I formally declare that the jointly published findings in both the thesis and the publication are greatly contributed by the candidate and were not or will not be used in the past or the future, respectively, for the purpose of acquiring an academic degree or title.

- High Spatiotemporal Resolution Analysis on Suspended Sediment and Microplastic Transport of a Lowland River. DOI: <https://doi.org/10.1016/j.scitotenv.2023.166188>

Szeged  
January 8<sup>th</sup>, 2024.

ALEXIA BALLA

A handwritten signature in black ink, appearing to read "Alexia Balla", written over a horizontal line.